Indonesian Journal of Electronics, Electromedical Engineering, and Medical Informatics e-ISSN: 2656-8624
Homepage: https://ijeeemi.org/; Vol. 7, No. 4, pp. 724-736, November 2025

RESEARCH PAPER

OPEN ACCES

Gait Variability and Phase Segmentation in Obese and Normal Individuals Using Multi-Location IMUs and Hidden Markov Models Supervised Marginal

Suto Setiyadi[1,2], Husneni Mukhtar[1,2], Willy Anugrah Cahyadi[1,2], Diyah Widiyasari[1], Mohamad Ramdhani[1], and Nigel Bryan Tang[1]

[1] Department School of Electrical Engineering, Telkom University, Bandung, Indonesia
[2] Laboratory of Advanced Biomedical Intelligent Engineering, Telkom University, Bandung, Indonesia

Abstract

Obesity is known to disrupt motor control and biomechanics; however, detailed gait alterations in individuals with obesity remain underexplored, particularly in dynamic and real-world walking conditions. This study aims to quantitatively characterize gait differences between individuals with obesity and those of normal weight by analyzing postural and temporal gait parameters. The investigation focuses on pitch, roll, and cadence dynamics using body-worn inertial sensors, with phase transition modeling via Hidden Markov Models. This work proposes a novel framework that integrates multi-location Inertial Measurement Unit (IMU) sensors and a Hidden Markov Model–Supervised Marginal (HMM-SM) approach to detect and classify gait phases with high accuracy, offering practical value for clinical gait assessment and personalized rehabilitation. IMU sensors were placed on the waist, thigh, calf, and heel to record gait data from participants in both obese and normal-weight groups. Gait segmentation and phase modeling were conducted using 4-, 5-, and 8-state HMMs. Quantitative analysis revealed significantly greater postural variability in the obese group during slow walking, with standard deviations in roll and pitch reaching 20.68° and 9.23°, respectively, much higher than the normal-weight group (0.60° and 0.26°). HMM-SM using 4, 5, and 8-state configurations captured gait phase distributions. For the 8-state model, obese participants showed higher average log-likelihood than normal-weight participants for pitch and roll during slow walking. However, Cross-Condition Robustness analysis showed a large drop in log-likelihood when the slow-walking-trained model was applied to fast walking, indicating limited adaptability. Effect sizes (Cramér's V) were largest for roll (V = 0.71) and moderate for pitch (V = 0.36–0.50) and cadence (V = 0.22–0.44). These results indicate that obesity increases postural variability and alters gait phase distributions, with intra-condition stability but reduced inter-condition adaptability. HMM-SM effectively quantifies temporal gait dynamics, offering a probabilistic framework for analyzing postural control differences.

Paper History
Received August 10, 2025
Revised October 21, 2025
Accepted November 5, 2025
Published November 10, 2025

Keywords
Obesity;
Gait Analysis;
Inertial Measurement Unit;
Hidden Markov Model Supervised Marginal;
Postural Stability

Author Email
Sutosetiyadisod @telkomuniversity.ac.id
Husnenimukhtar @telkomuniversity.ac.id
Waczze @telkomuniversity.ac.id
Diyahwidiyasari @telkomuniversity.ac.id
Mohamadramdhani @telkomuniversity.ac.id
Nigelbryan@student .telkomuniversity.ac.id

I. Introduction

Gait analysis is fundamental in assessing motor function, postural stability, and guiding rehabilitation interventions [1]. A typical gait cycle comprises a sequence of biomechanical phases representing body movement during ambulation. Broadly, this cycle is divided into two primary phases: the stance phase (approximately 60% of the cycle), where the foot maintains contact with the ground, and the swing phase (approximately 40%), during which the foot moves forward in preparation for the next step. Each of these phases can be further broken down into sub-phases, as illustrated in Fig. 1 [2], [3].

One demographic that presents unique gait challenges is individuals with obesity. Increased body mass, musculoskeletal strain, and neuromotor compensations in this group often result in altered gait patterns, decreased stability, and reduced walking efficiency [1], [4], [5]. These biomechanical changes increase the risk of falls, fatigue, and chronic joint disorders, making gait monitoring particularly important for this population [6].

Despite the clinical relevance, detailed investigations into how obesity affects dynamic gait parameters particularly pitch, roll, and cadence across multiple body segments remain scarce [7], [8]. Traditional gait analysis tools, such as optical motion capture systems, though accurate, are constrained by high costs, immobility, and the need for controlled lab conditions [7], [9]. In contrast, Inertial Measurement Units (IMUs) offer a portable, cost-effective solution for capturing spatiotemporal and kinematic data in real-world environments [10], [11].

Previous IMU-based research has predominantly focused on macro-level gait descriptors (e.g., stride length, walking speed). However, fine-grained analysis of segmental pitch and roll, particularly in obese populations, remains limited [12]. Moreover, the use of Hidden Markov Models (HMMs) for automatic gait phase recognition in

Corresponding author: Suto Setiyadi, sutosetiyadisod@telkomuniversity.ac.id, Department School Electrical Engineering, Jl. Telekomunikasi No. 1, 40257, Bandung, Indonesia.
Digital Object Identifier (DOI): https://doi.org/10.35882/ijeeemi.v7i4.269

such populations is still emerging, with insufficient empirical validation [13].

HMMs have demonstrated strong performance in segmenting gait phases using multi-sensor IMU data, outperforming earlier statistical methods like thresholding, Gaussian Mixture Models (GMM), Linear Discriminant Analysis (LDA), and Dynamic Time Warping (DTW) [14], [15]. Recent variants such as Supervised HMMs and the Supervised Marginal HMM (HMM-SM) have shown robustness in real-world applications and high correlation with clinical gait quality indicators [16], [17].

This study aims to evaluate gait characteristics in individuals with obesity and those of normal body weight using Inertial Measurement Unit (IMU) sensors placed at four anatomical locations: the waist, thigh, calf, and heel. Data from ten participants (five in each group) were analysed to extract biomechanical parameters, including pitch, roll, and cadence [9], [18]. Additionally, gait phase

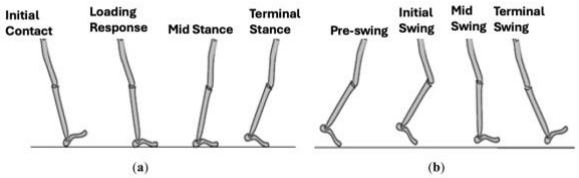

Fig. 1. The gait cycle is divided into two main parts: (a) the stance phase, occupying approximately 60% of the duration, characterised by the foot maintaining ground contact and carrying body weight; and (b) the swing phase, covering the remaining 40%, when the foot is elevated and moves ahead to initiate the subsequent step.

classification was performed using the Hidden Markov Model–Supervised Marginal (HMM-SM) approach, addressing the limitations of previous methods that relied solely on conventional statistical classifiers [15], [17], [19].

By comparing sensor data across groups and body segments, this study seeks to uncover biomechanical adaptations associated with obesity. The findings are expected to support the development of personalised gait monitoring systems, enhance clinical assessment of gait disorders, and enable real-time gait phase detection through the integration of wearable technologies in everyday environments.

II. Method

This study employed a quantitative observational approach with a comparative design to analyse gait characteristics between individuals with obesity and those with normal body weight. This study involved minimal-risk procedures, requiring participants only to wear leg-mounted sensors secured with a textile adapter and to walk a few steps. No invasive or semi-invasive interventions were conducted. All participants received a written informed consent form outlining the study procedures, clarifying that the tasks posed no risks beyond those associated with normal walking, and affirming their right to withdraw at any time without consequences. Only individuals who provided written consent were enrolled. Inclusion criteria specified healthy adults without mobility impairments, with no additional exclusion criteria applied.

Ten adult male participants were recruited, comprising five individuals with a body mass index (BMI) categorised as obese and five with a normal BMI, based on specific inclusion criteria, including the absence of significant neurological or musculoskeletal disorders. The overall research workflow is illustrated in Fig. 2.

Fig. 2 outlines the research process, which consists of two main stages: data acquisition and data analysis. In the first stage, data acquisition, gait data were collected using Inertial Measurement Unit (IMU) sensors mounted at four anatomical locations: the waist (1), thigh (2), calf (3), and heel (4), with sensor modules configured via ESP32 microcontrollers, as depicted in Fig. 2(a). The data collection protocol included: a 10-second sensor calibration, 1 minute of relaxed standing, walking trials under either fast or slow conditions over a 72.4-meter path, followed by 1 minute of standing still. IMU signals were sampled at a rate of 2 milliseconds and recorded in numeric format as CSV files.

Fig. 2(a) illustrates the configuration of the IMU (MPU9250) sensor placement on the participant's right leg, comprising four key anatomical locations: the waist, thigh, calf, and heel [20], [21], [22], [23]. This sensor arrangement was designed to capture comprehensive lower-limb movement dynamics during walking.

The sensor on the waist captures central body movement, while sensors on the thigh and calf record segmental leg motion related to swing and stance phases. The heel-mounted sensor plays a crucial role in detecting critical gait events such as heel strike and toe-off. This configuration enables the accurate acquisition of orientation data (pitch and roll) and temporal features, such as cadence, for gait analysis. Fig. 2(a) presents the embedded system configuration consisting of two ESP32 modules operating as a client-server pair. The ESP32 client reads data from four MPU9250 sensors via a TCA9548A I²C multiplexer, allowing for channel expansion, and transmits the signals over Bluetooth Low Energy (BLE) to the ESP32 server, which stores the data in CSV format. The recorded signals include acceleration, gyroscope, pitch, roll, and cadence from each participant.

As shown in Fig. 2(b), the collected data underwent a preprocessing stage that included merging data from five obese or normal participants, noise filtering using a low-pass filter, signal windowing with the root mean square (RMS) method, and signal normalisation. Feature selection was then performed to retain only the most relevant gait-related parameters: pitch, roll, and cadence. In the data analysis stage, this study employed Hidden Markov Models (HMMs) to identify gait phase patterns and to detect group differences between obese and normal participants. In addition, inferential statistical tests, including the Chi-square test, Mann–Whitney U test, and Cramér's V, were applied to assess the significance and effect size of the hidden state distributions. The HMM was trained over 200 iterations, assuming diagonal covariance for each hidden state (i.e., the variance of each feature was modelled independently of the others). The model consisted of eight states: State 0 = Initial Contact; State 1

Corresponding author: Suto Setiyadi, sutosetiyadisod@telkomuniversity.ac.id, Department School Electrical Engineering, Jl. Telekomunikasi No. 1, 40257, Bandung, Indonesia.
Digital Object Identifier (DOI): https://doi.org/10.35882/ijeeemi.v7i4.269

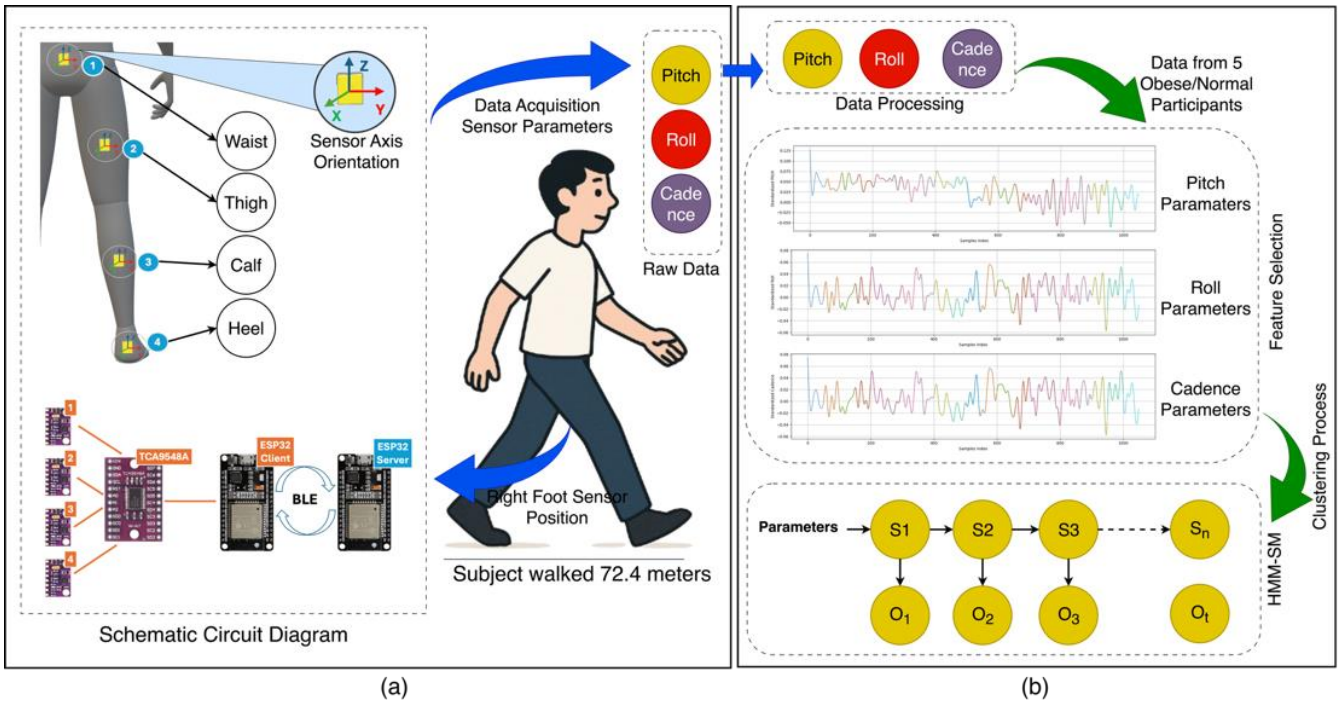

Fig. 2. Overview of the experimental setup and data processing pipeline using HMM for gait analysis: (a) Schematic of the wearable sensor system with IMUs placed on the waist, thigh, calf, heel, and foot to collect motion data during a walking task covering 72.4 meters; (b) Data analysis workflow, where raw sensor data (pitch, roll, and cadence) from five obese and five normal participants were processed into time-series signals, then modeled using a Hidden Markov Model Supervised Marginal (HMM-SM) to extract hidden gait states and classify gait patterns.

= Loading Response; State 2 = Midstance; State 3 = Terminal Stance; State 4 = Toe Off; State 5 = Initial Swing; State 6 = Midswing; State 7 = Terminal Swing as defined in Fig. 1.

Fig. 2(b) illustrates the workflow for training the Hidden Markov Model (HMM), which is used for segmenting gait phases based on pitch, roll, and cadence. The process begins with importing relevant libraries, such as Pandas (for data handling), Scikit-learn (for normalisation), and hmmlearn (for HMM implementation).

Data from all subjects (obese and normal), labelled according to walking speed (slow or fast), were combined and normalised using StandardScaler to ensure uniform scaling. A sliding window approach was employed to divide the time-series data into overlapping segments suitable for temporal modelling. Specifically, 21,434 samples (slow walking) and 13,440 samples (fast walking) were extracted using RMS feature extraction with a window size of 100 raw samples (~10 ms) at a sampling frequency of 50 Hz.

After preprocessing, HMMs were trained separately for each walking condition to identify the sequence of hidden states representing gait phases. The final step involves visualising the predicted state sequences and analysing state frequency distributions between slow and fast walking, which serves as the basis for comparing gait patterns between groups.

A. Inferential Statistical Testing

To evaluate differences in hidden state distributions between conditions (e.g., slow vs. fast walking), the Chi-square test was employed. This test determines the statistical significance of categorical distribution differences (states) based on the observed frequencies within each group. The basic formulation of the test is provided in Eq. (1) [24].

$$x^2 = \sum_{i=1}^{n} \frac{(O_i - E_i)^2}{E_i} \quad (1)$$

where x^2 is the Chi-square statistic, O_i indicates the frequency that was observed for the i-th category, E_i indicates the frequency that was expected for the i-th category, and n is the total number of categories in the contingency table [24].

In addition, Cramér's V was calculated to measure the effect size and express the association strength obtained from the Chi-square analysis, calculated as shown in Eq. (2) and with the interpretation of effect sizes provided in Table 1 [25].

$$V = \sqrt{\frac{x^2}{n(k-1)}} \quad (2)$$

Where V is the value of Cramér's V (ranging from 0 to 1), x^2 is the Chi-square statistic obtained from the contingency analysis, n indicates the overall sample size, and k corresponds to the lesser of the two dimensions, rows or columns, of the contingency table, i.e., $k = (r, c)$. To further evaluate the magnitude of association, Cramér's W (w) test was used in conjunction with Cramér's V to measure the effect size of discrepancies between observed and expected values, as illustrated in

Corresponding author: Suto Setiyadi, sutosetiyadisod@telkomuniversity.ac.id, Department School Electrical Engineering, Jl. Telekomunikasi No. 1, 40257, Bandung, Indonesia.
Digital Object Identifier (DOI): https://doi.org/10.35882/ijeeemi.v7i4.269

Table 1. Interpretation of Cramér's V/W values based on effect size. Values closer to 0 indicate weaker associations, while values exceeding 0.5 are considered strong.

V/W	Effect
0.0 ≤ V < 0.1	Weak (W)
0.1 ≤ V < 0.3	Small (L)
0.3 ≤ V < 0.5	Moderate (M)
≥0.5	Strong (S)

Eq. (3), with χ^2 signifying the Chi-square statistic and N the total sample count. The comparison of effect magnitudes is presented in Table 1 [25].

$$w = \sqrt{\frac{x^2}{N}} \quad (3)$$

B. Windowing Technique

The windowing technique is a signal processing method used to divide continuous or long-duration signals into short segments (windows), allowing for localised analysis in the time and/or frequency domain. This method is widely applied in the analysis of audio signals, physiological signals, and motion data obtained from Inertial Measurement Units (IMUs) for real-time feature extraction [26].

In this study, windowing was applied to cadence, pitch, and roll parameters recorded from IMU sensors, with Root Mean Square (RMS) employed as the feature extraction method for each windowed segment. RMS evaluates the magnitude of all signal values within a time window, regardless of polarity (positive or negative), making it suitable for oscillatory signals, such as body movement during walking. Higher RMS values reflect greater fluctuation or variability, particularly in parameters such as pitch (forward–backward tilt), roll (lateral tilt), and cadence (step frequency), which may indicate gait instability or irregularity.

A rectangular window function was used, as defined in Eq. (4), which assigns equal weight to all samples within a window. RMS values were calculated using Eq. (5) and later utilised to identify gait phases and analyse gait patterns [26], [27].

$$x_\omega[n] = x[n] \times \omega[n] \quad (4)$$

$$\mathrm{RMS}_k = \sqrt{\frac{1}{\mathrm{N}}\sum_{\mathrm{n}=0}^{\mathrm{N}-1} x_\omega[n]^2} \quad (5)$$

where $x[n]$ is the original signal, $\omega[n]$ is the window function, $x_\omega[\mathrm{n}]$ is the windowed signal, N is the window length (in samples), and RMS_k is the RMS value at the k-th window, representing the local signal energy.

C. IMU Based-Walking

The MPU9250 is a 9-axis Inertial Measurement Unit (IMU) sensor module that integrates three primary sensors within a single chip: an accelerometer, a gyroscope, and a magnetometer. The accelerometer captures linear acceleration in three orthogonal directions: x, y, and z, and the gyroscope captures angular velocity or rotation (pitch, roll) [28].

The roll ($\emptyset$) and pitch (θ) angles are computed based on acceleration components along the x, y, and z axes using the arctangent function, as defined in Eq. (6) and Eq. (7). Specifically, $\emptyset$ represents the object's rotation about the y-axis, which corresponds to the pitch (e.g., upward or downward motion of the front part of the body). a_x, a_y, and a_z are the acceleration values along the respective axes. The arctangent function (inverse tangent) is used to derive angles (in radians or degrees) from known tangent values [29], [30].

$$\emptyset = \arctan\left(\frac{a_y}{a_z}\right) \quad (6)$$

$$\theta = \arctan\left(\frac{-a_x}{\sqrt{a_y^2+a_z^2}}\right) \quad (7)$$

Step count (Eq. 8) and step duration are fundamental quantitative parameters in gait analysis used to assess step frequency and the time required to complete a single step cycle. These parameters reflect the degree of temporal regulation and postural stability during walking. In contrast, step length and cadence describe the spatial and rhythmic aspects of gait, which are closely associated with locomotor efficiency and the integrity of neuromuscular control. Here, A_{mag} represents the total acceleration magnitude, and a_x, a_y, a_z are the acceleration components along the x, y, and z axes [31], [32].

$$A_{mag} = \sqrt{a_x^2 + a_y^2 + a_z^2} \quad (8)$$

$$cadence = \frac{Step\ Count}{Step\ Duration} \times 60 \quad (9)$$

Cadence, expressed in steps per minute (SPM), indicates an individual's movement rhythm. Higher cadence values correspond to faster gait or running rhythms. It is computed by dividing the total number of steps by the duration of the walking activity and converting it to a per-minute unit, as shown in Eq. (9) [32].

D. Hidden Markov Model (HMM)

In this study, the Hidden Markov Model (HMM) was employed to identify gait phases based on orientation and rhythm parameters, namely pitch, roll, and cadence. HMM is a probabilistic model widely used in sequential data processing and dynamic systems involving hidden states. Within gait analysis, HMM effectively detects transitions between gait phases, such as heel strike, foot flat, mid-stance, heel-off, and swing phase, which cannot be directly observed but can be inferred from sensor data [19].

The HMM was trained using pitch, roll, and cadence data collected from participants. Once trained, the model automatically segmented gait cycles based on sequences of observations. This approach can manage signal irregularities and inter-individual variability and has been extensively applied in IMU-based gait studies [33].

The model comprises three fundamental components: the state transition probability matrix A, as represented in Eq. (10); the emission probability function B, as shown in Eq. (11); and the initial state probability distribution π, as expressed in Eq. (12).

$$a_{ij} = P\left(q_{t+1} = s_j \middle| q_t = s_i\right) \quad (10)$$

$$b_j(o_t) = P\left(o_t \middle| q_t = s_j\right) \quad (11)$$

$$\mathbf{\Pi}_j = P(q_1 = s_i) \quad (12)$$

Corresponding author: Suto Setiyadi, sutosetiyadisod@telkomuniversity.ac.id, Department School Electrical Engineering, Jl. Telekomunikasi No. 1, 40257, Bandung, Indonesia.
Digital Object Identifier (DOI): https://doi.org/10.35882/ijeeemi.v7i4.269

To determine the most probable sequence of gait phases given the observed data, the Viterbi algorithm was used to compute the optimal hidden state sequence $Q^* = \{q_1, q_2, \dots, q_n\}$ algorithm that maximises the joint probability $P(Q|O\lambda)$, where $\lambda = (A, B, \pi)$ represents the HMM model parameters [19].

Using the HMM-SM technique, gait phases were automatically classified based on IMU-measured pitch, roll, and cadence values, where the phases (heel strike to terminal swing) correspond to hidden states defined in Eq. (13). At the same time, the observed multivariate features at time o_t are described as in Eq. (14).

$$S = \{s_1, s_2, \dots, s_n\} \quad (13)$$

$$\boldsymbol{o_t} = [\theta_t + \emptyset_t + \boldsymbol{cadence_t}]^t \quad (14)$$

The HMM performance was assessed using K-Fold Cross-Validation and Cross-Condition Robustness Testing. In K-fold validation, data are split into K equal folds. The model is trained on K–1 and tested on the remaining fold, with the process repeated for each fold to measure generalisation and consistency. The average log-likelihood across all iterations is then used to evaluate the consistency of the model parameters across different data partitions. A minor variance among folds indicates a more stable HMM that is less prone to overfitting to specific subsets.

Meanwhile, the Cross-Condition Robustness Test was applied to evaluate the model's ability to maintain performance when applied to data conditions that differ from those used during training. In this study, the HMM trained on slow walking conditions was tested on fast walking data, and vice versa. Robustness was quantified based on the log-likelihood values computed from cross-condition data. A high log-likelihood value indicates that the state transition patterns and observation distributions learned by the model remain relevant even when walking conditions change. Therefore, these two evaluation approaches complement each other in assessing the reliability of the HMM, both in terms of internal stability (through cross-validation) and adaptability across conditions (through cross-condition robustness) [34].

III. Results

This study analysed pitch, roll, and cadence data recorded from IMU sensors during walking to assess gait patterns and postural stability quantitatively. Variability analysis was conducted using the mean (μ) and standard deviation (σ) to evaluate postural steadiness and step consistency. Variability analysis was conducted using the mean (μ) and standard deviation (σ) to evaluate postural steadiness and step consistency.

Compared to normal-weight participants, obese individuals exhibited more dispersed pitch and roll distributions, particularly during slow walking, evidenced by wider interquartile ranges, more outliers, and extreme roll values (maximum: 138.33°, minimum: −128.28°), with standard deviations of 20.68° for roll and 9.23° for pitch during slow walking that decreased significantly to 0.60° and 0.31°, respectively, during fast walking, while normal-weight participants showed narrower interquartile ranges, fewer outliers, and lower variability (roll: 0.60° slow, 0.54° fast; pitch: 0.26° slow, 0.30° fast), suggesting better postural control, which was also supported by cadence analysis wherein obese participants showed increased median cadence from slow to fast walking but retained a wide data spread (max cadence: 181.82 SPM slow, 171.43 SPM fast; SD: 55.05 and 52.08 SPM), whereas normal-weight participants demonstrated more symmetrical cadence distributions with fewer outliers and more minor standard deviations (52.38 SPM slow, 38.68 SPM fast), indicating greater step rhythm consistency at higher walking speeds.

To automatically identify gait phases, the extracted data were analysed using the Hidden Markov Model with Supervised Marginal (HMM-SM). This model identified walking phases based on the probabilistic patterns of the three gait parameters, capturing temporal dynamics while accommodating inter-individual variability. The results were visualised through state transition probabilities and gait phase classifications. The analysis was conducted separately for obese and normal-weight participants using an eight-state model representing gait phases (based on Fig. 1), from Initial Contact (State 0) to Terminal Swing (State 7), as illustrated in Fig. 3.

Fig. 3 presents the classification of hidden gait states using the Supervised Marginal Hidden Markov Model (HMM-SM) across three parameters, pitch, roll, and cadence, in obese and normal participants under slow (blue) and fast (red) walking conditions, using an 8-state HMM over 2,000 samples. Fig. 3 was analysed using Cramér's W to examine deviations of the distribution from a uniform pattern based on Eq. (3) and Table 1.

The results presented in Fig. 3 for the obese group indicate that the chi-square test revealed a significant deviation of the HMM state distribution based on the pitch parameter from a uniform pattern under both slow (χ^2 = 22007.05, $p < 0.001$, w = 1.01) and fast (χ^2 = 1308.41, $p < 0.001$, w = 0.28) walking conditions. These findings suggest that the pitch angle does not vary evenly throughout the gait cycle but is instead dominated by specific phases. During slow walking, the distribution showed a strong dominance of State 4 (37.1%), followed by State 7 (23.6%) and State 0 (23.1%), reflecting prolonged periods with relatively small and stable pitch angles within limited phases. Conversely, during fast walking, the proportions across states became more balanced, with a marked increase in State 2 (17.6%), State 6 (16.9%), and State 7 (15.5%). This shift indicates greater variability in the pitch angle at higher walking speeds Furthermore, for the obese participants, the chi-square test revealed that the HMM state distribution based on the roll parameter significantly deviated from a uniform distribution under both slow (χ^2 = 22,388.34, $p < 0.001$, w = 1.02) and fast (χ^2 = 1,066.89, $p < 0.001$, w = 0.25) walking conditions. These results confirm that variations in the roll angle (lateral body inclination) during the gait cycle were not evenly distributed but concentrated within certain phases. During slow walking, the distribution was dominated by State 0 (29.8%) and State 5 (31.6%), followed by State 7 (25.1%), reflecting a tendency toward high lateral stability, where the roll angle remained relatively constant.

Corresponding author: Suto Setiyadi, sutosetiyadisod@telkomuniversity.ac.id, Department School Electrical Engineering, Jl. Telekomunikasi No. 1, 40257, Bandung, Indonesia.
Digital Object Identifier (DOI): https://doi.org/10.35882/ijeeemi.v7i4.269

Table 2. Statistical comparison of hidden state distribution (8-Class, 4-Class, & 5-Class HMM-SM) with Cramér's V effect between obese and normal groups during slow and fast walking conditions. (W = Weak, L = Small, M = Moderate, and S = Strong).

Group	Parameters	8-State			4-State			5-State		
		χ^2	V	Effect	χ^2	V	Effect	χ^2	V	Effect
Slow	Pitch	3460.05	0.36	M	6601.40	0.50	S	5481.00	0.45	M
	Roll	13181.47	0.71	S	4129.08	0.39	M	10699.28	0.64	S
	Cadence	1212.49	0.22	L	4619.14	0.42	M	2731.77	0.32	M
Fast	Pitch	5476.75	0.42	M	3865.23	0.35	M	3966.56	0.36	M
	Roll	2836.93	0.30	M	1221.04	0.19	L	1014.70	0.18	L
	Cadence	5321.16	0.42	M	6095.83	0.44	M	4625.12	0.38	M

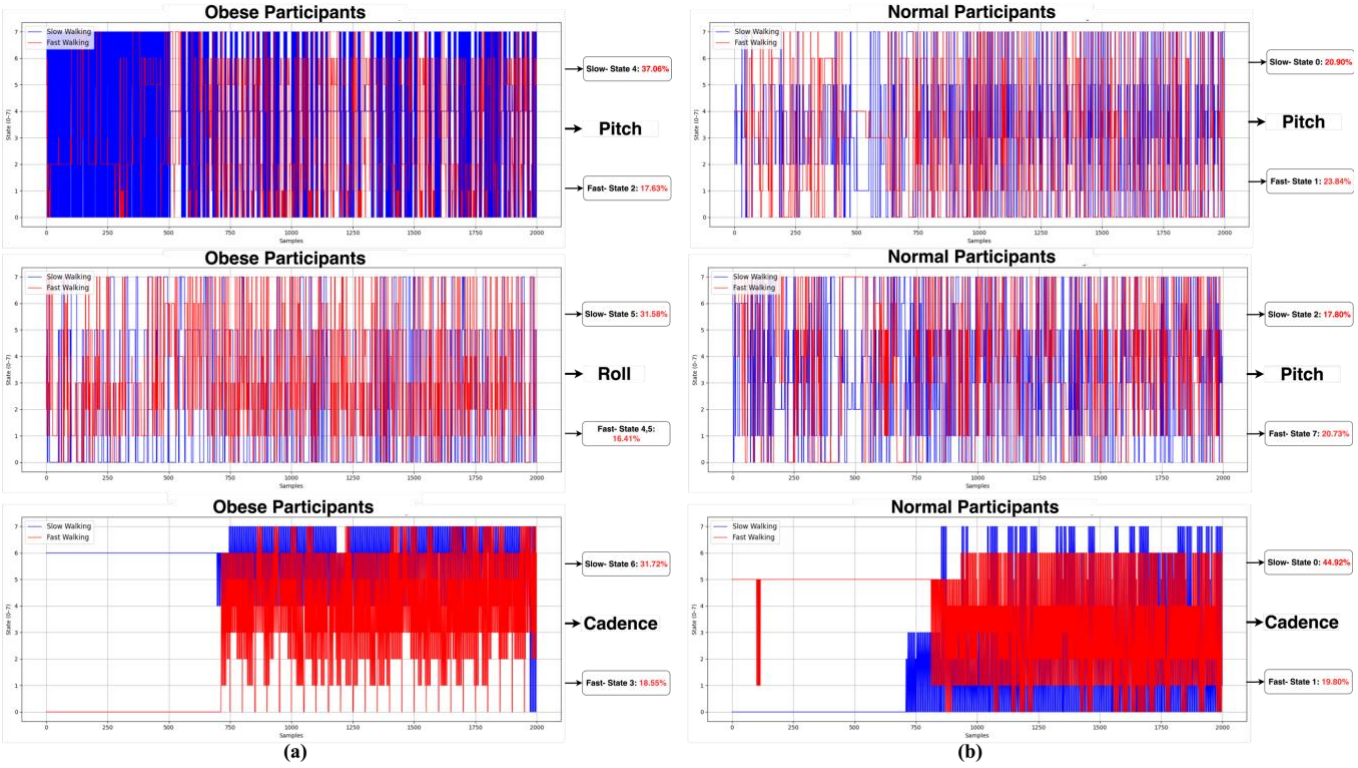

Fig. 3. HMM-SM hidden state activation for the parameters pitch, roll, and cadence (from top to bottom) during slow (blue) and fast (red) walking for Obese participants and Normal participants.

As walking speed increased, the distribution became more uniform and shifted toward higher proportions in States 2 (13.3%), 4 (16.4%), and 5 (16.4%), indicating greater lateral rotational activity during step-to-step transitions.

For the cadence parameter in obese participants, the chi-square test showed that the HMM state distribution based on cadence significantly deviated from a uniform distribution under both slow (χ^2 = 12,060.96, $p < 0.001$, w = 0.75) and fast (χ^2 = 2,597.80, $p < 0.001$, w = 0.39) walking conditions. This suggests that variations in step rhythm (frequency or cadence) were not evenly distributed throughout the gait cycle, but rather concentrated in specific phases. During slow walking, State 6 dominated the distribution (31.7%), followed by State 7 (22.0%) and State 4 (15.4%), reflecting periods characterised by a more extended and stable step rhythm. As walking speed increased, the distribution became more dispersed and shifted toward higher proportions in States 0 (18.0%), 3 (18.6%), and 6 (18.2%).

In normal participants (Fig. 3), the chi-square test showed that the HMM state distribution based on the pitch parameter significantly deviated from a uniform distribution under both slow (χ^2 = 860.39, $p < 0.001$, w = 0.43) and fast (χ^2 = 5,166.17, $p < 0.001$, w = 0.62) walking conditions. These results confirm that changes in pitch angle throughout the gait cycle were not evenly distributed but concentrated in specific phases. During slow walking, the distribution was relatively balanced, dominated by States 0 (20.9%) and 3 (16.4%), followed by States 7 (15.5%) and 5 (14.5%), reflecting stable pitch variations. As walking speed increased, the distribution shifted markedly, with substantial increases in State 1 (23.8%), State 3 (20.6%), and State 0 (20.6%), accompanied by sharp decreases in State 7 (3.7%) and State 5 (4.1%).

Corresponding author: Suto Setiyadi, sutosetiyadisod@telkomuniversity.ac.id, Department School Electrical Engineering, Jl. Telekomunikasi No. 1, 40257, Bandung, Indonesia.
Digital Object Identifier (DOI): https://doi.org/10.35882/ijeeemi.v7i4.269

This shift indicates an increased dynamic behaviour of pitch rotation.

For the roll parameter in normal participants, the chi-square test showed that the HMM state distribution based on the roll parameter significantly deviated from a uniform distribution under both slow (χ^2 = 296.60, $p < 0.001$, w = 0.26) and fast (χ^2 = 2,780.18, $p < 0.001$, w = 0.46) walking conditions. This finding suggests that variations in the roll angle (lateral body inclination) during the gait cycle were not random but rather concentrated in specific phases of the gait cycle. At slower walking speeds, the distribution was relatively balanced, with the highest proportions in State 2 (17.8%), followed by States 3 (14.2%), 4 (13.5%), and 7 (13.5%), suggesting stable lateral body control. As walking speed increased, the distribution shifted toward higher proportions in States 6 (18.4%) and 7 (20.7%), indicating greater lateral dynamics and more active body movement at higher speeds.

For the cadence parameter, the chi-square test revealed that the HMM state distribution based on cadence significantly deviated from a uniform distribution under both slow (χ^2 = 4,430.02, $p < 0.001$, w = 0.99) and fast (χ^2 = 3,970.58, $p < 0.001$, w = 0.54) walking conditions. This result indicates that step rhythm (frequency or cadence) was not randomly distributed but organised into distinct phase patterns throughout the gait cycle. At slower walking speeds, the distribution was highly uneven, with a strong dominance in State 0 (44.9%), reflecting efficient rhythmic control and high stability during slow walking. As walking speed increased, the HMM state distribution became more dispersed and balanced, with sharp increases in State 1 (19.8%), State 4 (19.5%), and State 5 (19.5%), indicating an increase in step frequency.

Further evaluation compared obese and normal participants by examining the Cramér's V effect size to assess differences in the hidden state distribution between obese and normal participants during slow and fast walking, as presented in Table 2, with effect sizes varying across parameters. Additionally, Table 2 presents the evaluation results for obese and normal participants using two different models: the 4-class and 5-class models.

Table 2 presents the statistical comparison of hidden state distributions obtained from three HMM configurations (8-state, 4-state, and 5-state HMM-SM) between obese and normal participants during slow and fast walking conditions, analysed using the chi-square (χ^2) test and Cramér's V effect size. Overall, the results indicate that the obese group exhibited more substantial deviations in hidden state distributions across several gait parameters, particularly under slow walking conditions.

For the pitch parameter, the 8-state model yielded a moderate effect size (V = 0.36), which increased to a strong effect (V = 0.50) in the 4-state model, suggesting that reducing model complexity enhanced the discrimination of dominant postural transitions between groups. The roll parameter, representing mediolateral body motion, showed the strongest group differentiation in the 8-state model (V = 0.71), indicating that obese participants had more pronounced lateral oscillations, likely as a compensatory strategy to maintain balance during slow walking. In contrast, the cadence parameter showed moderate effects (V = 0.22–0.42), reflecting rhythmic gait differences that were less pronounced than those observed in postural parameters. Under fast walking conditions, the pitch parameter maintained a moderate effect (V = 0.42–0.47), while the roll parameter demonstrated a decrease in effect size (V = 0.30–0.34), suggesting reduced postural differentiation between groups as dynamic balance demands increased. The cadence parameter also showed moderate but consistent effects (V = 0.38–0.44), indicating persistent rhythmic differences between groups at higher walking speeds.

In the 8-class Hidden Markov Model (HMM), the analysis of the pitch parameter produced a higher average log-likelihood value for the obese group (5420.55 ± 416.22) compared to the normal group (–1354.61 ± 55.76) under slow walking conditions. This indicates that the 8-class HMM was able to represent the postural transition patterns of obese participants more effectively. However, the Cross-Condition Robustness test revealed a substantial decrease in log-likelihood when the model trained on slow walking data was tested on fast walking data (Obese = –19504.53; Normal = –2538.49), suggesting limited adaptability of the model to dynamic speed changes. For the roll parameter, which reflects lateral body motion, the 8-class model also showed a higher average log-likelihood for the obese group (6404.20 ± 367.73) than for the normal group (–1740.88 ± 48.85). Nevertheless, the Cross-Condition Robustness results again indicated a marked decline (Obese = –20155.81; Normal = –3338.89), implying that while obese participants exhibit consistent lateral movement patterns, these patterns are less flexible under varying gait speeds. The cadence parameter analysis within the same 8-class HMM model further supported these findings. Obese participants demonstrated a more stable step rhythm under slow walking conditions (mean = 6577.54 ± 605.96) compared to fast walking (mean = 1640.90 ± 2031.36). The Cross-Condition Robustness analysis reinforced this trend, with a sharp performance drop when models were tested across conditions.

The comparison between obese and normal participants in the 4-state model revealed apparent differences in gait pattern stability. For the *pitch* parameter, the obese group exhibited a higher positive average log-likelihood (5420.55 ± 416.22) during slow walking compared to the normal group (–1354.61 ± 55.76). Similarly, for the *roll* parameter, the obese group showed a higher log-likelihood value (6404.20 ± 367.73) than the normal group (–1740.88 ± 48.85). Meanwhile, the *cadence* parameter indicated that obese participants had a more stable and predictable step rhythm (log-likelihood = 5297.41 ± 173.21 during slow walking) compared to normal participants (–2128.95 ± 1281.50).

The five-state HMM analysis revealed distinct differences in gait dynamics between obese and normal participants across pitch, roll, and cadence parameters. For the pitch parameter, the obese group exhibited substantially higher model stability under slow-walking

Corresponding author: Suto Setiyadi, sutosetiyadisod@telkomuniversity.ac.id, Department School Electrical Engineering, Jl. Telekomunikasi No. 1, 40257, Bandung, Indonesia.
Digital Object Identifier (DOI): https://doi.org/10.35882/ijeeemi.v7i4.269

conditions (average log-likelihood = 5420.55 ± 416.22) compared to the normal group (–1354.61 ± 55.76). However, model generalisation across conditions declined sharply, as indicated by the Cross-Condition Robustness test (Obese = –18038.68; Normal = –787.86), suggesting a reduced adaptability of pitch dynamics to increased walking speed. The roll parameter demonstrated a similar trend. The obese group showed higher model stability during slow walking (6404.20 ± 367.73) than the normal group (–1740.88 ± 48.85), suggesting enhanced lateral compensatory control. Yet, performance decreased significantly when tested across conditions (Obese = –18993.15; Normal = –3169.35), highlighting limited adaptability in mediolateral trunk control with changing gait speeds. For the cadence parameter, the obese group displayed more consistent and predictable rhythmic patterns, reflected in higher log-likelihood values during slow walking (6604.87 ± 768.50) compared to the normal group (–826.39 ± 1201.53). This stability persisted, though reduced, in the fast-walking condition (1551.46 ± 126.10 vs. –953.19 ± 1208.12). Nonetheless, cross-condition testing revealed a substantial deterioration in performance for both groups (Obese: –52,736 to –70,362; Normal: –58,845 to –41,288).

IV. Discussion

The distribution of pitch and roll indicates that obese participants exhibited significantly higher postural variability compared to normal-weight participants, particularly during slow walking. This finding aligns with previous studies suggesting that obesity negatively affects neuromotor control and increases body oscillations during gait [35], [36]. The wide interquartile range and elevated standard deviation in the obese group can be interpreted as compensatory strategies to address instability or biomechanical constraints [36], [37]. Conversely, the more concentrated and symmetrical patterns observed in the normal group suggest efficient postural control and better adaptation to changes in walking speed.

In addition to obesity, various other factors have been reported to influence gait patterns, including ageing, muscle weakness, sensorimotor impairments, and musculoskeletal conditions. Ageing, for example, is associated with a decline in proprioceptive function and muscle strength, which may increase step variability and the risk of imbalance [38]. Neurological impairments, such as Parkinson's disease and peripheral neuropathy, are also associated with altered gait characteristics due to disrupted motor coordination and postural control [39]. Moreover, environmental factors such as floor surface type and footwear use can affect gait stability and postural compensation strategies [40]. Therefore, although obesity is a significant determinant in this study, the interpretation of the findings should also account for the contributions of other external and physiological factors.

Furthermore, the significant effect size values (Cramér's V) reflect the degree of gait control reorganisation. Obese participants exhibited generally high V values (V > 0.5), particularly for the pitch and roll parameters, indicating substantial deviations in distribution patterns and a reduction in gait stability. This suggests increased postural variability and compensatory strategies in both the sagittal and mediolateral planes. In contrast, normal participants showed smaller and more consistent V values (V < 0.3), reflecting stable state transitions and preserved motor control. The enormous effect size observed in the cadence parameter among obese participants also indicates altered temporal coordination, associated with reduced rhythmic regularity and increased energetic demands during walking [41]. The findings highlight that the obese group displayed greater alterations in postural stability and gait rhythm, particularly under slow walking conditions. The 8-state model effectively captured complex postural variability (notably in roll), whereas the 4-state model emphasised dominant gait transitions (notably in pitch). These results align with previous biomechanical evidence suggesting that obesity increases postural variability and reduces adaptive control during gait [42].

Furthermore, building on earlier investigations that employed Hidden Markov Models (HMM) with fewer than six states for gait phase detection [43], [44]. The study assesses the Supervised Marginal HMM in two structural setups comprising four and five states, respectively. The four-state version includes Initial Contact, Terminal Stance, Initial Swing, and Terminal Swing. In contrast, the five-state version provides finer segmentation of the stance phase into Initial Contact, Loading Response, Mid Stance, Terminal Stance, and Swing Phase. As shown in Table 2, these findings demonstrate that obese participants exhibit higher intra-condition gait stability but lower inter-condition adaptability, particularly in the pitch and roll dimensions. The 8-state model captured more nuanced postural variability, whereas the 4- and 5-state models emphasised dominant gait transitions. Collectively, these results suggest that obesity is associated with increased postural rigidity and reduced dynamic adaptability, reflecting altered neuromuscular control strategies that prioritise stability over flexibility.

From a clinical standpoint, this pattern of increased intra-condition stability but decreased adaptability may underlie functional gait impairments commonly observed in individuals with obesity. The reduced ability to modulate trunk and limb dynamics across varying walking speeds or perturbations has been associated with diminished reactive balance capacity and an elevated risk of falls. This biomechanical rigidity, particularly in the mediolateral and sagittal planes, can limit compensatory adjustments during transitions or unexpected disturbances, thereby compromising gait safety and efficiency [45], [46], [47].

The selection of state cardinality in HMM-SM should be adjusted according to the particular needs of the intended application. Models with fewer states provide greater efficiency and high classification accuracy for the principal gait phases. In contrast, the eight-state model offers a more detailed representation of postural transitions, albeit with a modest reduction in overall accuracy. However, the gait sub-phases detected by HMM-SM do not yet fully align with the sequential order of

Corresponding author: Suto Setiyadi, sutosetiyadisod@telkomuniversity.ac.id, Department School Electrical Engineering, Jl. Telekomunikasi No. 1, 40257, Bandung, Indonesia.
Digital Object Identifier (DOI): https://doi.org/10.35882/ijeeemi.v7i4.269

actual gait sub-phases, as illustrated in the Fig. 3. Furthermore, the generalizability of this study is limited, as the dataset included only 10 participants (5 obese and five normal), all male, which constrains the broader applicability of the findings.

V. Conclusion

This study examined gait parameters in obese and normal-weight participants using IMU sensors placed on the waist, thigh, calf, and heel. The analysis revealed significant variations in pitch, roll, and cadence across the two groups. Obese participants exhibit significantly higher postural variability than normal-weight participants, as indicated by σ values (pitch: 9.23° vs 0.26° slow; roll: 20.68° vs 0.54° slow) and interquartile ranges. The HMM-SM model effectively captures gait phase distributions, showing higher average log-likelihood for obese participants (pitch: 5420.55 ± 416.22; roll: 6404.20 ± 367.73) during slow walking. Effect sizes (Cramér's V) reveal substantial deviations in postural control for roll (V = 0.71) and moderate deviations for pitch (V = 0.36–0.50) and cadence (V = 0.22–0.44). Cross-condition robustness analysis demonstrates a decrease in log-likelihood across speeds (obese pitch: −19,504.53; normal: −2,538.49), indicating limited adaptability under dynamic conditions. Overall, obesity is associated with increased postural rigidity and reduced dynamic adaptability, reflecting altered neuromuscular strategies that prioritise stability over flexibility. HMM-SM provides a quantitative, probabilistic framework for comparing gait phase patterns. These findings suggest that obesity exerts a considerable effect on the stability and temporal structure of gait. The IMU-based HMM-SM method effectively identified subtle gait patterns and holds potential for automated monitoring, especially in obese individuals. Study limitations include a small sample size (n = 10), restricted walking conditions, and a lack of clinical validation. Future work should involve diverse participants, real-world settings, and clinical comparisons with predictive models to enhance the understanding of the phenomenon.

References

[1] J. L. Perez-Lasierra, M. Azpíroz-Puente, J. V. Alfaro-Santafé, A. J. Almenar-Arasanz, J. Alfaro-Santafé, and A. Gómez-Bernal, "Sarcopenia screening based on the assessment of gait with inertial measurement units: a systematic review," *BMC Geriatr*, vol. 24, no. 1, Dec. 2024, doi: 10.1186/s12877-024-05475-3.

[2] W. Tao, T. Liu, R. Zheng, and H. Feng, "Gait analysis using wearable sensors," Feb. 2012. doi: 10.3390/s120202255.

[3] A. Kharb, V. Saini, Y. K. Jain, and S. Dhiman, "A review of gait cycle and its parameters," 2011. [Online]. Available: www.IJCEM.orgIJCEMwww.ijcem.org

[4] M. B. del Rosario, S. J. Redmond, and N. H. Lovell, "Tracking the evolution of smartphone sensing for monitoring human movement," Jul. 31, 2015, *MDPI AG*. doi: 10.3390/s150818901.

[5] R. Monfrini, G. Rossetto, E. Scalona, M. Galli, V. Cimolin, and N. F. Lopomo, "Technological Solutions for Human Movement Analysis in Obese Subjects: A Systematic Review," Mar. 01, 2023, *MDPI*. doi: 10.3390/s23063175.

[6] J. B. Dingwell and L. C. Marin, "Kinematic variability and local dynamic stability of upper body motions when walking at different speeds," *J Biomech*, vol. 39, no. 3, pp. 444–452, 2006, doi: 10.1016/j.jbiomech.2004.12.014.

[7] G. Prisco *et al.*, "Validity of Wearable Inertial Sensors for Gait Analysis: A Systematic Review," Jan. 01, 2025, *Multidisciplinary Digital Publishing Institute (MDPI)*. doi: 10.3390/diagnostics15010036.

[8] S. K. Manna, M. A. Hannan Bin Azhar, and A. Greace, "Optimal locations and computational frameworks of FSR and IMU sensors for measuring gait abnormalities," Apr. 01, 2023, *Elsevier Ltd*. doi: 10.1016/j.heliyon.2023.e15210.

[9] Y. He *et al.*, "Accuracy validation of a wearable IMU-based gait analysis in healthy female," *BMC Sports Sci Med Rehabil*, vol. 16, no. 1, Dec. 2024, doi: 10.1186/s13102-023-00792-3.

[10] A. Muro-de-la-Herran, B. García-Zapirain, and A. Méndez-Zorrilla, "Gait analysis methods: An overview of wearable and non-wearable systems, highlighting clinical applications," Feb. 19, 2014. doi: 10.3390/s140203362.

[11] S. Lin *et al.*, "A Review of Gait Analysis Using Gyroscopes and Inertial Measurement Units," Jun. 01, 2025, *Multidisciplinary Digital Publishing Institute (MDPI)*. doi: 10.3390/s25113481.

[12] A. Khumar and B. Kumar, "SVM based Multiclass Classifier for Gait phase Classification using Shank IMU Sensor," 2017.

[13] L. Liu *et al.*, "Ambulatory human gait phase detection using wearable inertial sensors and Hidden Markov model," *Sensors (Switzerland)*, vol. 21, no. 4, pp. 1–24, Feb. 2021, doi: 10.3390/s21041347.

[14] M. Sánchez-Manchola, L. Arciniegas-Mayag, M. Múnera, M. Bourgain, T. Provot, and C. A. Cifuentes, "Effects of stance control via hidden Markov model-based gait phase detection on healthy users of an active hip-knee exoskeleton," *Front Bioeng Biotechnol*, vol. 11, 2023, doi: 10.3389/fbioe.2023.1021525.

[15] M. D. S. Manchola, M. J. P. Bernal, M. Munera, and C. A. Cifuentes, "Gait phase detection for lower-limb exoskeletons using foot motion data from a single inertial measurement unit in hemiparetic individuals," *Sensors (Switzerland)*, vol. 19, no. 13, Jul. 2019, doi: 10.3390/s19132988.

[16] Y. Wang, Q. Song, T. Ma, N. Yao, R. Liu, and B. Wang, "Research on Human Gait Phase Recognition Algorithm Based on Multi-Source Information Fusion," *Electronics (Switzerland)*, vol.

Corresponding author: Suto Setiyadi, sutosetiyadisod@telkomuniversity.ac.id, Department School Electrical Engineering, Jl. Telekomunikasi No. 1, 40257, Bandung, Indonesia.
Digital Object Identifier (DOI): https://doi.org/10.35882/ijeeemi.v7i4.269

12, no. 1, Jan. 2023, doi: 10.3390/electronics12010193.

[17] G. Ng and J. Andrysek, "Hidden Markov model-based similarity measure (HMM-SM) for gait quality assessment of lower-limb prosthetic users using inertial sensor signals," *J Neuroeng Rehabil*, vol. 22, no. 1, Dec. 2025, doi: 10.1186/s12984-025-01638-4.

[18] S. Sharif Bidabadi, I. Murray, and G. Y. F. Lee, "Validation of foot pitch angle estimation using inertial measurement unit against marker-based optical 3D motion capture system," *Biomed Eng Lett*, vol. 8, no. 3, pp. 283–290, Aug. 2018, doi: 10.1007/s13534-018-0072-5.

[19] J. Taborri, S. Rossi, E. Palermo, F. Patanè, and P. Cappa, "A novel HMM distributed classifier for the detection of gait phases by means of a wearable inertial sensor network," *Sensors (Switzerland)*, vol. 14, no. 9, pp. 16212–16234, Sep. 2014, doi: 10.3390/s140916212.

[20] S. Lee, C. Park, E. Ha, J. Hong, S. H. Kim, and Y. Kim, "Determination of Spatiotemporal Gait Parameters Using a Smartphone's IMU in the Pocket: Threshold-Based and Deep Learning Approaches," *Sensors*, vol. 25, no. 14, p. 4395, Jul. 2025, doi: 10.3390/s25144395.

[21] L. Tang, M. Shushtari, and A. Arami, "IMU-Based Real-Time Estimation of Gait Phase Using Multi-Resolution Neural Networks," *Sensors*, vol. 24, no. 8, Apr. 2024, doi: 10.3390/s24082390.

[22] R. Stenger, H. H. Pour, J. Teich, A. Hein, and S. Fudickar, "Gait Parameters Estimation from Sensor-Belt IMU Data," Jul. 30, 2024. doi: 10.36227/techrxiv.172235876.62229016/v1.

[23] T. Liu, Y. Inoue, and K. Shibata, "Development of a wearable sensor system for quantitative gait analysis," *Measurement (Lond)*, vol. 42, no. 7, pp. 978–988, Aug. 2009, doi: 10.1016/j.measurement.2009.02.002.

[24] V. S., H. A.S, and J. S. Sundar, "CHI-SQUARE TESTS: A QUICK GUIDE FOR HEALTH RESEARCHERS," *Int J Adv Res (Indore)*, vol. 12, no. 10, pp. 1214–1222, Oct. 2024, doi: 10.21474/IJAR01/19746.

[25] M. L. McHugh, "The Chi-square test of independence," *Biochem Med (Zagreb)*, vol. 23, no. 2, pp. 143–149, 2013, doi: 10.11613/BM.2013.018.

[26] A. Phinyomark, R. N. Khushaba, and E. Scheme, "Feature extraction and selection for myoelectric control based on wearable EMG sensors," *Sensors (Switzerland)*, vol. 18, no. 5, May 2018, doi: 10.3390/s18051615.

[27] W. Caesarendra and T. Tjahjowidodo, "A review of feature extraction methods in vibration-based condition monitoring and its application for degradation trend estimation of low-speed slew bearing," Dec. 01, 2017, *MDPI AG*. doi: 10.3390/machines5040021.

[28] V. Suvorkin, M. Garcia-Fernandez, G. González-Casado, M. Li, and A. Rovira-Garcia, "Assessment of Noise of MEMS IMU Sensors of Different Grades for GNSS/IMU Navigation," *Sensors*, vol. 24, no. 6, Mar. 2024, doi: 10.3390/s24061953.

[29] A. M. Sabatini, "Estimating three-dimensional orientation of human body parts by inertial/magnetic sensing," Feb. 2011. doi: 10.3390/s110201489.

[30] A. J. L. H. R. V. Sebastian O.H. Madgwick, *Estimation of IMU and MARG orientation using a gradient descent algorithm*. IEEE, 2011.

[31] J. S. Sheu, W. C. Jheng, and C. H. Hsiao, "Implementation of a three-dimensional pedometer automatic accumulating walking or jogging motions in arbitrary placement," *Int J Antennas Propag*, vol. 2014, 2014, doi: 10.1155/2014/372814.

[32] R. A. Brindle, J. B. Taylor, C. Rajek, A. Weisbrod, and K. R. Ford, "Association Between Temporal Spatial Parameters and Overuse Injury History in Runners: A Systematic Review and Meta-analysis," Feb. 01, 2020, *Springer*. doi: 10.1007/s40279-019-01207-5.

[33] C. Voisard, N. de l'Escalopier, D. Ricard, and L. Oudre, "Automatic gait events detection with inertial measurement units: healthy subjects and moderate to severe impaired patients," *J Neuroeng Rehabil*, vol. 21, no. 1, Dec. 2024, doi: 10.1186/s12984-024-01405-x.

[34] A. Yamashita *et al.*, "Harmonization of resting-state functional MRI data across multiple imaging sites via the separation of site differences into sampling bias and measurement bias," *PLoS Biol*, vol. 17, no. 4, 2019, doi: 10.1371/journal.pbio.3000042.

[35] J. Rekant, S. Rothenberger, and A. Chambers, "Obesity-Specific Considerations for Assessing Gait with Inertial Measurement Unit-Based vs. Optokinetic Motion Capture," *Sensors*, vol. 24, no. 4, Feb. 2024, doi: 10.3390/s24041232.

[36] C. W. Frames *et al.*, "Dynamical properties of postural control in obese community-dwelling older adults," *Sensors (Switzerland)*, vol. 18, no. 6, Jun. 2018, doi: 10.3390/s18061692.

[37] M. Pau, P. Capodaglio, B. Leban, M. Porta, M. Galli, and V. Cimolin, "Kinematics adaptation and inter-limb symmetry during gait in obese adults," *Sensors*, vol. 21, no. 17, Sep. 2021, doi: 10.3390/s21175980.

[38] B. Bogen, R. Moe-Nilssen, M. K. Aaslund, and A. H. Ranhoff, "Muscle Strength as a Predictor of Gait Variability after Two Years in Community-Living Older Adults," *Journal of Frailty and Aging*, vol. 9, no. 1, pp. 23–29, Jan. 2020, doi: 10.14283/jfa.2019.24.

[39] M. Reina-Bueno *et al.*, "Effect of foot orthoses and shoes in parkinson's disease patients: A prisma systematic review," Nov. 01, 2021, *MDPI*. doi: 10.3390/jpm11111136.

[40] A. L. Simon, V. Lugade, K. Bernhardt, A. N. Larson, and K. Kaufman, "Assessment of stability during

Corresponding author: Suto Setiyadi, sutosetiyadisod@telkomuniversity.ac.id, Department School Electrical Engineering, Jl. Telekomunikasi No. 1, 40257, Bandung, Indonesia.
Digital Object Identifier (DOI): https://doi.org/10.35882/ijeeemi.v7i4.269

gait in patients with spinal deformity A preliminary analysis using the dynamic stability margin," *Gait Posture*, vol. 55, pp. 37–42, Jun. 2017, doi: 10.1016/j.gaitpost.2017.03.036.

[41] T. E. Lockhart, C. W. Frames, R. Soangra, and A. Lieberman, "Effects of Obesity and Fall Risk on Gait and Posture of Community-Dwelling Older Adults."

[42] O. Hue *et al.*, "Body weight is a strong predictor of postural stability," *Gait Posture*, vol. 26, no. 1, pp. 32–38, Jun. 2007, doi: 10.1016/j.gaitpost.2006.07.005.

[43] G. Ng, A. Gouda, and J. Andrysek, "Quantifying Asymmetric Gait Pattern Changes Using a Hidden Markov Model Similarity Measure (HMM-SM) on Inertial Sensor Signals," *Sensors*, vol. 24, no. 19, Oct. 2024, doi: 10.3390/s24196431.

[44] G. Ng and J. Andrysek, "Hidden Markov model-based similarity measure (HMM-SM) for gait quality assessment of lower-limb prosthetic users using inertial sensor signals," *J Neuroeng Rehabil*, vol. 22, no. 1, Dec. 2025, doi: 10.1186/s12984-025-01638-4.

[45] T. E. Lockhart, C. W. Frames, R. Soangra, and A. Lieberman, "Effects of Obesity and Fall Risk on Gait and Posture of Community-Dwelling Older Adults."

[46] P. C. Desrochers, D. Kim, L. Keegan, and S. V Gill, "Association between the Functional Gait Assessment and spatiotemporal gait parameters in individuals with obesity compared to normal weight controls: A proof-of-concept study." [Online]. Available: http://www.ismni.org.

[47] Z. F. Lerner, W. J. Board, and R. C. Browning, "Effects of obesity on lower extremity muscle function during walking at two speeds," Gait Posture, vol. 39, no. 3, pp. 978–984, 2014, doi: 10.1016/j.gaitpost.2013.12.020.

Author Biography

Suto Setiyadi obtained his Bachelor of Engineering (S.T.) degree from Telkom University in 2021 and subsequently received his Master of Engineering (M.T.) degree from the same university in 2023. His research activities began at the Microprocessor and Interface Laboratory and the Electronics Laboratory. After completing his undergraduate studies, he worked as a research assistant at Bandung Techno Park. Following his master's graduation, he continued his academic career as a lecturer and researcher at the School of Electrical Engineering, Telkom University, Indonesia. He authored the textbook Sensor and Actuator with the Cases of Implementation (Tel-U Press, 2022). His primary research interests include biomedical applications of computer vision and embedded systems.

Husneni Mukhtar obtained her Ph.D. from the Doctoral School of Electronics, Microelectronics, and Photonics at the Université de Strasbourg, France 2018. After completing his research at the ICube Laboratory – CNRS–Unistra, France, she began his academic career as a lecturer and researcher at the School of Electrical Engineering, Telkom University, Indonesia. She subsequently led the Renewable Energy and Advanced Electronics Engineering Laboratory (2020–2023) and founded the Advanced Biomedical Intelligent Engineering Laboratory in 2022. She authorises several academic textbooks, including Sensor and Actuator with the Cases of Implementation (Tel-U Press, 2022) and Biomedical Physics (Tel-U Press, 2024). Her main research interests include image processing instrumentation for industrial inspection and biomedical analysis, nanometrology, and 3D optical profilometry. She also develops instrumentation and control applications across various engineering domains.

Willy Anugrah Cahyadi is a lecturer in the Undergraduate Electrical Engineering Program at Telkom University, who earned his bachelor's and master's degrees in Electrical Engineering and Microelectronics from Institut Teknologi Bandung (ITB), and his doctoral degree (Dr. Eng.) in Information and Communications Engineering from Pukyong National University, South Korea; he is a member of the Control, Electronics & Intelligent System (CEIS) research group, focusing on Visible Light Communication (VLC), optical systems, body area networks, and signal processing, with over 60 publications and active involvement in research, curriculum development, and community service in intelligent electro-technological solutions.

Diyah Widiyasari received her bachelor's degree in electrical engineering from Institut Teknologi Sumatera in 2021 and her master's degree in electrical engineering from Institut Teknologi Bandung in 2023. She has been actively involved in research related to radar signal processing, embedded systems, and hardware design. Her current research interests include the development of signal processing algorithms for radar applications and hardware–software co-design.

Corresponding author: Suto Setiyadi, sutosetiyadisod@telkomuniversity.ac.id, Department School Electrical Engineering, Jl. Telekomunikasi No. 1, 40257, Bandung, Indonesia.
Digital Object Identifier (DOI): https://doi.org/10.35882/ijeeemi.v7i4.269

Mohamad Ramdhani is a lecturer in the Undergraduate Electrical Engineering program at Telkom University, specializing in control and electronics within the CEIS research group. He holds a bachelor's degree in electrical engineering from STT Telkom and a master's degree in electrical engineering from Institut Teknologi Bandung. His research interests include software implementation and microcontroller-based system design.

Nigel Bryan Tang is an undergraduate student in the Electrical Engineering program at Telkom University, Indonesia. He is currently active as a laboratory assistant in the Microprocessor and Interface Laboratory, where he is involved in practical sessions, providing technical assistance, and developing microcontroller-based and embedded system projects.

Corresponding author: Suto Setiyadi, sutosetiyadisod@telkomuniversity.ac.id, Department School Electrical Engineering, Jl. Telekomunikasi No. 1, 40257, Bandung, Indonesia.
Digital Object Identifier (DOI): https://doi.org/10.35882/ijeeemi.v7i4.269

Each author is required to provide a cover image as shown example below

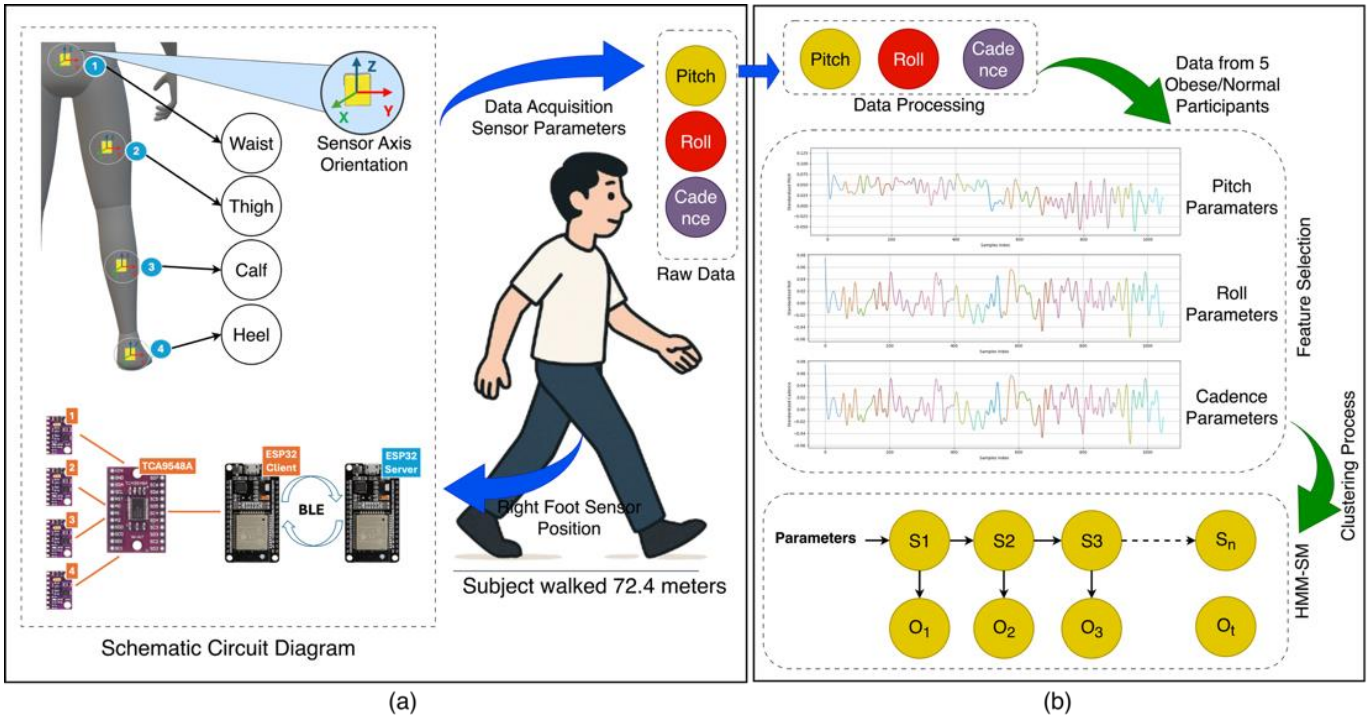

Corresponding author: Suto Setiyadi, sutosetiyadisod@telkomuniversity.ac.id, Department School Electrical Engineering, Jl. Telekomunikasi No. 1, 40257, Bandung, Indonesia.
Digital Object Identifier (DOI): https://doi.org/10.35882/ijeeemi.v7i4.269